The relationship between quantum spin glass and many-body localization

Brendan P. Marsh
Department of Applied Physics, Stanford University, Stanford, CA 94305
(Dated: January 8, 2021)

Submitted as coursework for PH470, Stanford University, Spring 2020

Disordered energy landscapes can give rise to distinctive phases of matter. The spin glass, a network of frustrated spins with random bonds, exhibits a low temperature, non-ergodic phase with all spins "frozen" in a complex metastable state. Many-body localized (MBL) quantum systems defy the usual expectation of interacting many-body systems to reach a state of thermal equilibrium, most often due to a disordered potential. The spin glass and MBL phases have qualitative similarities; both are characterized by a breakdown of the ergodic behavior on which the foundations of statistical mechanics rest. Are these two phases effectively equivalent in a model of a quantum spin glass? Here we explore the relationship between the phases in the explicit models of Kjäll *et al.* and Laumann *et al.*[1,2]. Both models show that the spin glass phase is accompanied by MBL, but that the MBL phase persists beyond the limit of the glass phase into paramagnetic phases.

I. INTRODUCTION

The spin glass and MBL phases share numerous qualitative features. In both phases, there is a breakdown of thermal behavior. In classical statistical mechanics this is associated with a breakdown of ergodic dynamics at the spin glass phase transition due to insurmountable free energy barriers. In the quantum realm, loss of thermal behavior arises due to many-body localization; eigenstates in the MBL phase are exponentially localized in space. In both cases, the system becomes effectively frozen. Moreover, disorded energy landscapes tend to play prominent roles in both phases.

In this paper, we discuss the extent to which the spin glass and MBL phases overlap, and to what extent one phase implies the other. Our findings compile the results of two studies which have probed models that demonstrate both phases. These are the disordered transverse field Ising model[1] and the quantum random energy model[2]. A simplified summary of the forthcoming analysis is illustrated in Fig. 1, showing the overlap between the spin glass and MBL phase in the two models. In words, we find that the full spin glass phase has demonstrated MBL in both models, with the MBL phase extending past the glassy phase into the paramagnetic phase. Thus, while the phases are qualitatively similar, the precise location of their phase boundaries prove to be quantitatively different in these models.

The paper is structured as follows. In Sec. II, we review the basic notions of a spin glass and the order parameters that we will use to quantify the glassy phase. This is followed by a brief introduction to quantum statistical mechanics and MBL in Sec. III. The focus of this section is to define what it means for a closed quantum system to display effectively thermal behavior, and conversely what it means for a quantum state to be many-body localized. With the necessary background material covered, the disordered transverse field Ising model is presented in Sec. IV. The half-chain entanglement entropy is introduced as an indicator of the MBL phase, culminating in the phase diagram presented in Fig. 5. The quantum random energy model is presented in Sec. V, with a derivation of the free energy in the classical random energy model followed by the spectral diagnostics used to study the quantum model. This yields the full phase diagram in Fig. 7. We conclude with a brief discussion of the common trends seen in the two models.

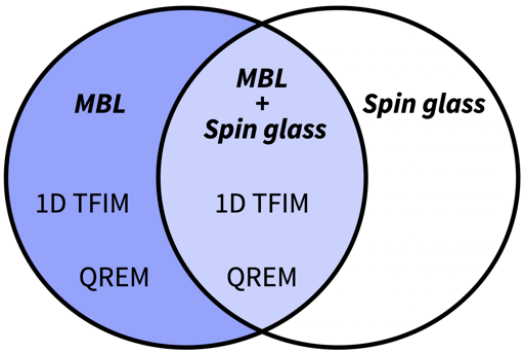

FIG. 1: A Venn diagram summarizing the relationship between the spin glass and many-body localized phases in models studied here. Both the disordered 1D transverse field Ising model (1D TFIM)[1] and the quantum random energy model (QREM)[2] demonstrate both an MBL phase without spin glass order, and a phase with both MBL and spin glass order. Neither model shows a phase with spin glass order in the absence of MBL.

II. SPIN GLASS

The world feels very cold to silicon dioxide, the primary constituent of the glass in our window panes. At temperatures below about 850 K, silicon dioxide undergoes a *glass* transition from a viscous liquid state to a frozen state with a rigid, amorphous solid structure. The resulting glass has no well-defined periodic structure, unlike the crystalline structures seen in materials like typical metals and insulators. Periodic structure forms the backbone of solid state physics, and without it, our usual methods like Bloch's theorem simply do not apply. Without the tools of traditional solid state theory, glass can be a challenging material to understand.

A *spin* glass is similar in spirit to a physical glass. It is composed of a set of spin degrees of freedom, which, below a critical temperature, organize into a complex and highly non-uniform metastable state. For clarity, we can compare a spin glass with the familiar ferromagnet. In the ferromagnetic, each spin minimizes the total energy by aligning with its neighboring spins. In a spin glass, however, there is a random mixture of ferromagnetic and antiferromagnetic interactions between spins. Below the critical temperature, the ferromagnet orders with all spins aligned, whereas the spin glass organizes into a complicated state that minimizes the free energy.

A defining feature of spin glasses is their inability to find a ground state which simultaneously minimizes the energy of each bond between spins. This phenomenon does not occur in the ferromagnet or antiferromagnet, and is referred to as *frustration*. This can be demonstrated with as few as three classical spins, constrained to point up or down. When two of the three pairs of spins have a ferromagnetic interaction, while the final pair has an antiferromagnetic interaction, there is no state of the spins which can simultaneously minimize the energy of each bond. This is illustrated in Fig. 2 for both a triplet of frustrated spins, and a larger set of spins with random bonds as seen in the archetypal Sherrington-Kirkpatrick model of a spin glass[3]. Frustration often leads to degenerate ground states with energies higher than those in unfrustrated systems.

A generic model that encapsulates many common spin glass models is described by the Hamiltonian

$$H = -\sum_{i,j=1}^{N} J_{ij} s_i \cdot s_j, \tag{1}$$

where s_i is the ith spin, which can be modelled as either classical dipoles or quantum spin-1/2 operators, and the sum runs over all spins from 1 to N. The couplings J_{ij} contain quenched disorder, meaning they are chosen randomly but are fixed for a given system. Spins for which $J_{ij} > 0$ experience ferromagnetic interactions while $J_{ij} < 0$ indicates antiferromagnetic interactions. If the sum is restricted to nearby neighboring spins then the Hamiltonian describes the Edwards-Anderson model[4]. Often, the spins are restricted to align along a single axis

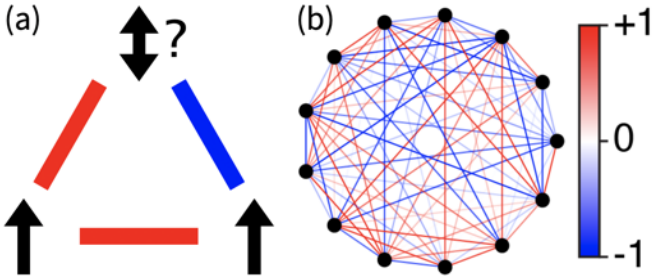

FIG. 2: Connectivity in a spin glass. (a) A frustrated triplet of spins, where red (blue) bonds denote ferromagnetic (antiferromagnetic) coupling. To satisfy the lower bond, the bottom spins align. However, this leaves the top spin in a "frustrated" state in which it cannot satisfy both of its bonds. (b) A typical connectivity graph between 13 spins in the Sherrington-Kirkpatrick model[3]. Positive red bonds denote ferromagnetic coupling while negative blue bonds denote antiferromagnetic coupling. The ground state is highly frustrated and challenging to find.

and can be represented by the states $s_i = (1, 0)^T$ for spin up and $s_i = (0, 1)^T$ for spin down. The Hamiltonian can then be written as

$$H = -\sum_{i,j=1}^{N} J_{ij} \sigma_i^z \cdot \sigma_j^z, \tag{2}$$

where σ_i^z is the Pauli operator. This general Hamiltonian has a $\mathbb{Z}_2$ symmetry operator $P = \prod_{i=1}^{N} \sigma_i^x$ that flips all spins, so that $[H, P] = 0$. When the J_{ij} couplings are infinite-range, independently and identically distributed Gaussian random variables, this Hamiltonian describes the Sherrington-Kirkpatrick model[3].

Precise analytical description of spin glasses and their thermodynamic properties is a notoriously challenging task that has entertained physicists and mathematicians for at least the last half of a century. However, a simple quantitative description of the spin glass phase can be understood in terms of order parameters that mark the presence of spin glass order. The typical order parameter used to describe spin glass order is the static Edwards-Anderson (EA) order parameter[4]. This is defined as

$$q_{\text{EA}} \equiv \langle \langle \sigma_i^z \rangle_T^2 \rangle_J \tag{3}$$

where an arbitrary individual spin has been chosen corresponding to a particular i. The inner average $\langle \cdot \rangle_T$ denotes a time average over states as the system evolves at temperature T, while the outer average $\langle \cdot \rangle_J$ denotes an average over realizations of the quenched disorder in the J couplings. There are various technical difficulties with this form of the EA order parameter, but it captures the basic notion of a breakdown in ergodicity in the system. To see this, recall the $\mathbb{Z}_2$ symmetry of the Hamiltonian which flips every spin. If every spin can be simultaneously flipped without changing the energy, then in an ergodic system, the time spent in any given state

will be equal to the time spent in the all spins flipped version of the state. This implies that in an ergodic system, the net magnetization $\langle\sigma_i^z\rangle_T$ should be identically zero for every spin so that $q_{\rm EA} = 0$. However, if the dynamics are non-ergodic, the system does not fully explore the state space and it is no longer required that the net magnetization of any spin be zero. This allows for a nonzero spin glass order parameter $q_{\rm EA} > 0$. Physically, this is achieved when the temperature is sufficiently low so that large free energy barriers separate the low energy metastable states from each. Thermal fluctuations are then insufficient to drive ergodic behavior (at least on any observable timescale).

A related order parameter that can be derived from $q_{\rm EA}$ diverges at the spin glass transition. Suppose a small, random magnetic field H_i is applied at each site to bias each spin with mean magnitude $\langle H_i^2\rangle_J = H^2$. The *spin glass susceptibility* is then defined as

$$\chi_{\rm SG} \equiv (k_B T^2)\frac{d}{dH^2} q_{\rm EA}. \tag{4}$$

For our model in Eqn. (2), it can be shown from linear response theory that $\chi_{\rm SG}$ takes the form[5]

$$\chi_{\rm SG} = \frac{1}{N}\sum_{i,j=1}^{N} \left\langle \left(\langle\sigma_i^z\sigma_j^z\rangle_T - \langle\sigma_i^z\rangle_T\langle\sigma_j^z\rangle_T\right)^2\right\rangle_J. \tag{5}$$

In the paramagnetic phase, the individual magnetizations disappear, leaving only the correlations between spins. At the spin glass transition, the system becomes frozen into a metastable state so that the spins become fully correlated and $\chi_{\rm SG} \propto N$ diverges in the thermodynamic limit. Thus, the susceptibility acts a sensitive indicator of the spin glass transition.

III. MANY-BODY LOCALIZATION

Many-body localization can be regarded as a failure of the standard thermalizing behavior that is both expected for many-body interacting systems and required to justify the use of quantum statistical mechanics. As such, to understand MBL we require an understanding of these concepts. In this section, we build these concepts starting from the basics of quantum theory.

Beginning with textbook quantum mechanics, we recall that a quantum state is described by a vector, which in the notation of Dirac takes the name "ket", and is written as $|\psi\rangle$. The vector space in which these kets live is called the Hilbert space $\mathcal{H}$, which contains every quantum state that the system can exist in. Given some observable $\mathcal{O}$, represented mathematically as a hermitian operator on the space of quantum states, the expected value of $\mathcal{O}$ is found via the inner product $\langle\mathcal{O}\rangle \equiv \langle\psi|\,\mathcal{O}\,|\psi\rangle$. However, in quantum statistical mechanics, the main objects of interest are not single quantum states but thermodynamic *ensembles* of states. Ensembles are most conveniently represented in the density matrix formalism, in which quantum states are represented as operators themselves. The density matrix of a pure state $|\psi\rangle$ is $\rho = |\psi\rangle\langle\psi|$, which is, in words, the outer product of the vector $|\psi\rangle$. The expectation value of the observable $\mathcal{O}$ then becomes

$$\langle\rho\rangle = \mathrm{Tr}(\mathcal{O}\rho). \tag{6}$$

The advantage of the density matrix formalism is that it allows for simple construction of ensembles of pure states. Namely, given a collection of pure states $|\psi_i\rangle$ which occur with probabilities p_i, the density matrix describing the ensemble is simply $\rho = \sum_i p_i\,|\psi\rangle\langle\psi|$. From the normalization of probability, $\sum_i p_i = 1$, we see that the density matrix is normalized so that $\mathrm{Tr}\,\rho = 1$. Finally, the *purity* of the density matrix is defined as $\mathrm{Tr}\,\rho^2$, which is unity for pure states and less than unity for mixed states containing multiple pure states.

To develop a theory of quantum statistical mechanics, quantum analogs of classical thermodynamic ensembles can be defined. Given a Hamiltonian H, which we take to be time independent, there exist eigenstates $|\psi_i\rangle$ with associated energy eigenvalues E_i. The *microcanonical ensemble* of states with some energy E is defined as

$$\rho_{\rm mc}(E) = \frac{1}{N_{\rm mc}}\sum_{i=1}^{N_{\rm mc}} |\psi_i\rangle\langle\psi_i|\,, \tag{7}$$

where the sum is taken over the number $N_{\rm mc}$ of states $|\psi_i\rangle$ with energies E_i in the range $E\pm\Delta E/2$. The width of the energy window ΔE should be made small so that only states of nearly equal energy are included in the ensemble. In words, the microcanonical ensemble is an equally weighted probability distribution of quantum states with approximately equal energies.

The *canonical ensemble* is defined not directly by an energy but by a temperature T. This ensemble models interaction of the system with a thermal bath exchanging energy with the system. For convenience, we often work with the inverse temperature defined as $\beta = 1/(k_B T)$, where k_B is the Boltzmann constant. Then, the canonical ensemble is constructed as

$$\rho_{\rm can}(\beta) = \frac{1}{Z}\exp(-\beta H), \tag{8}$$

where $Z = \sum_i e^{-\beta E_i}$ is the same partition function as used in classical statistical mechanics. The above form involving a matrix exponential can be simplified by writing the Hamiltonian in terms of its energy eigenstates as $H = E_i\,|\psi\rangle\langle\psi|$. Then, by expanding the matrix exponential as a Taylor series, it is straightforward to show that the canonical ensemble takes the simpler form

$$\rho_{\rm can}(\beta) = \frac{1}{Z}\sum_i e^{-\beta E_i}\,|\psi_i\rangle\langle\psi_i|\,. \tag{9}$$

There is a certain equivalence for the canonical and microcanonical ensembles in the thermodynamic limit,

so that $\langle\mathcal{O}\rangle_{\rm mc}(E_0) = \langle\mathcal{O}\rangle_{\rm can}(T)$ when there is a specific relation between E_0 and T. For a system of fixed volume the energy and temperature are related through the fundamental thermodynamic relation,

$$\frac{1}{T} = \frac{dS}{dE}, \tag{10}$$

where S is the entropy of the system. Explicitly, it can be written as $S = k_B \log\Omega$, where Ω is the number of microscopic states of the system that are consistent with a given set of macroscopic quantities. Using this relation, it can be shown that the microcanonical ensemble with energy E_0 and canonical ensemble with temperature T produce the same expectation values under the condition

$$\langle H\rangle_{\rm can} = \frac{1}{Z}\sum_i E_i e^{-E_i/k_BT}. \tag{11}$$

To describe the ensembles of quantum states that we have defined, we must measure some observable. Many-body localization is concerned with the behavior of local observables, being those which describe the properties of only a small subsystem. Local observables are often the simplest kind of observable to measure experimentally, such as the value of a spin at a particular point in the system. To define local observables quantitatively, we must partition the full system, described by a Hilbert space $\mathcal{H}$, into two subsystems A and B, with Hilbert spaces $\mathcal{H}_A$ and $\mathcal{H}_B$. A local observable can then be described as an operator with the form $\mathcal{O} = \mathcal{O}_A \otimes I_B$, where I_B is the identity operator on $\mathcal{H}_B$. For such a local observable, we can show that the expectation value of $\mathcal{O}$ depends only on a reduced form of the density matrix. Specifically, a few lines of linear algebra shows that

$$\mathrm{Tr}((\mathcal{O}_A \otimes I_B)\rho) = \mathrm{Tr}_A(\mathcal{O}_A\rho_A), \tag{12}$$

where ρ_A is called the *reduced* density matrix and is defined using the partial trace over subsystem B as $\rho_A = \mathrm{Tr}_B\,\rho$.

Finally, we are equipped to understand what it means for a quantum state $|\psi\rangle$ to be thermal. We again consider a general density matrix ρ, which may be a pure state, a partition of the full Hilbert space into a small subsystem A and larger subsystem B, and a local observable $\mathcal{O}$. The density matrix ρ is said to be effectively thermal if

$$\mathrm{Tr}_B\,\rho = \mathrm{Tr}_B\,\rho_{\rm mc}(E_0). \tag{13}$$

That is, if the expectation value of a general local observable $\mathcal{O}$ is equal for the state ρ and a microcanonical ensemble of states with energy E_0. Using the equivalence between the canonical and microcanonical ensembles, a similar definition could be given in terms of the canonical ensemble.

It is generically expected that in many-body interacting systems, generic initial states $|\psi(t=0)\rangle$ will eventually thermalize, so that as the time t becomes large Eqn. (13) will become true. Intuitively, this arises because the system is sufficiently large to act as its own heat bath for smaller subsystems, so that subsystems come into thermal equilibrium with rest of the system. In the case where $|\psi\rangle$ is an eigenstate of the Hamiltonian and $\rho = |\psi\rangle\langle\psi|$ is thermal state, this becomes the celebrated *eigenstate thermalization hypothesis*. In words, this states that single eigenstates of the Hamiltonian can act as legitimate thermodynamic ensembles for small subsystems.

Finally, the nature of many-body localized systems is precisely to *avoid* thermalization of this sort. That is, when an initial state $|\psi(t=0)\rangle$ does not eventually evolve to a thermal state, it is said to be a many-body localized state. As we will see, this is typically achieved by introducing a disordered energy landscape into the Hamiltonian, which causes spatial localization of the eigenstates in the same fashion as Anderson localization[6]. Indeed, MBL is nothing more than Anderson localization in the presence of interactions.

There is a phase transition between the MBL phase and the delocalized phase, aptly named the many-body localization-delocalization (MBLD) phase transition. However, growing evidence suggests that the MBLD transition is a dynamical phase transition which occurs at the level of individual eigenstates of the Hamiltonian, rather than an equilibrium transition. That is, nonanalytic changes occur in the structure of individual eigenstates as system parameters are tuned across a critical threshold that depends on the energy density of the eigenstate. This suggests that for a fixed Hamiltonian, there may exists some eigenstates that are in the MBL phase and others which are not. Indeed, this division has been seen numerically and is known as the many-body mobility edge.

IV. THE DISORDERED ISING CHAIN

With the basics of spin glass and MBL covered, we now turn our attention to specific models demonstrating these phases to see how they do or do not overlap with each other. The first system we review was studied by Kjäll et al.[1], and is composed of a 1D lattice of length L, with spin-1/2 degrees of freedom on each site. The spins experience Ising interactions between nearest neighbors and next-nearest neighbors. To endow the model with quantum dynamics, a uniform transverse field is added. The Hamiltonian describing the system is

$$H = -\sum_{i=1}^{L-1} J_i\sigma_i^z\sigma_{i+1}^z + J_2\sum_{i=1}^{L-2}\sigma_i^z\sigma_{i+2}^z + h\sum_i^L\sigma_i^x. \tag{14}$$

The nearest neighbor interactions have the form $J_i = J+\delta J_i$, where each δJ_i is a random variable chosen from a uniform distribution on the interval $[-\delta J, \delta J]$. This term provides the disorder that is crucial to the MBL phase. In the current study, the dimensionless parameters were fixed to $J = 1$ and $h/2 = J_2 = 0.3$. Like the generic model of a spin glass introduced in Eqn.2, there is a global

$\mathbb{Z}_2$ symmetry corresponding to the parity operator $P = \prod_{i=1}^{L} \sigma_i^x$ which flips every spin.

To build intuition for the dynamics of the system, first consider the limit of $\delta J = J_2 = 0$, being the standard transverse field Ising model. There is a ferromagnetic phase ($J > h$) characterized by the ground state $|\downarrow \cdots \downarrow\rangle + |\uparrow \cdots \uparrow\rangle$, and a quantum paramagnet phase ($J < h$) with ground state $|\rightarrow \cdots \rightarrow\rangle$ where $|\rightarrow\rangle = (|\uparrow\rangle - |\downarrow\rangle)/\sqrt{2}$. In the ferromagnetic phase, excitations of the system look like domain walls separating ferromagnetic regions, e.g. the state $|\uparrow\uparrow\uparrow\downarrow\downarrow\rangle$ with a domain wall between the second and third sites. In the absence of disorder, states with the same number of domain walls are degenerate, thus allowing for delocalized superpositions of states with domain walls at any location. The effect of on-site disorder, setting $\delta J > 0$, is to exponentially localize the location of domain walls in the chain. Finally, turning on the next-nearest neighbor interaction $J_2 > 0$ introduces repulsive interactions between domain walls. This interaction, in contrast to on-site disorder, drives thermalization.

Many-body localization is probed via the entanglement entropy of eigenstates. Given an arbitrary partition of the physical system into two subsystems A and B, for example dividing the lattice into a left half (A) and right half (B), the entanglement entropy of a quantum state with density matrix ρ is

$$S = -\mathrm{Tr}_A\left[\rho_A \ln(\rho_A)\right], \tag{15}$$

where $\rho_A = \mathrm{Tr}_B\, \rho$ is the reduced density matrix on A. The entanglement entropy is a robust tool for differentiating between thermal and many-body localized states. It is well-established[7] that many-body localized eigenstates show an entanglement entropy that scales with the area of the boundary between between subregions A and B, while thermal states show larger entanglement entropy that scales with a volume law, being the total size of subsystem A rather than its perimeter. Thus, as the disorder is increased, the MBLD transition should manifest itself in the form of a transition from large entanglement entropy scaling with the system size in the thermal phase to small entanglement entropy independent of system size in the MBL phase. This behavior is verified in Fig. 3a, in which we numerically compute the entanglement entropy for the model.

To identify the location of the actual MBLD transition between these two phases, the authors consider two similar measures. The first is σ_S, the standard devation of the entanglement entropy for the eigenstate closest in energy to a fixed energy E, averaged over disorder realizations. Deep in either the thermal of localized phase, all eigenstates are expected to follow either volume law or area law, without strong fluctuations. Thus, away from the transition, σ_S should be small. On the other hand, near the MBLD transition, it is possible that some eigenstates may fall on thermal side of the transition and others on the localized side of the transition. Thus, in computing σ_S, there will be fluctations in S between volume law and are law, so σ_S should be expected to peak near the MBLD transition. Indeed this is the case, as shown in Fig. 3 near a disorder strength of about $\delta J \approx 2$.

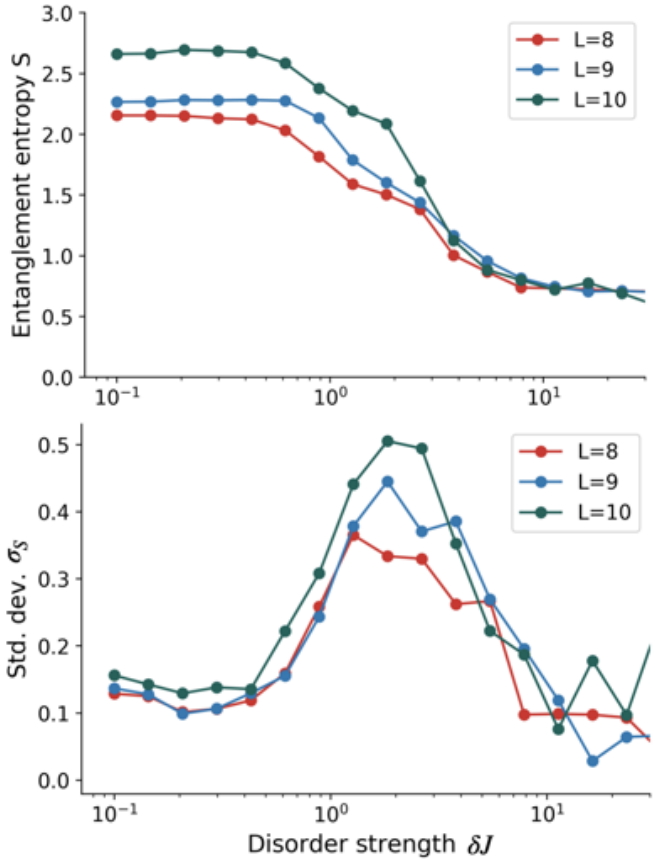

FIG. 3: The half-chain entanglement entropy S (a) and standard deviation σ_S (b) in the disordered transverse field Ising model. System sizes $L = 8, 9, 10$ were probed. The entanglement entropy was computed for eigenvectors near the middle of the spectrum, corresponding to the infinite temperature limit, and averaged over many realizations of quenched disorder.

A qualitatively similar indicator of the MBLD transition comes from performing a quantum quench of an initially pure eigenstate $|n\rangle$. That is, $|n\rangle$ is first perturbed by flipping the first spin. The state, now a mixture of eigenstates, is then allowed to evolve under unitary dynamics until the entanglement entropy $S_n(t)$ of the state saturates at long times. The difference in entanglement entropy,

$$\Delta S_n \equiv S_n(t) - S_n(0), \tag{16}$$

is then used as another indicator of the MBLD transition. This can be understood by again considering the limiting cases. In thermal phase, small perturbations have only a small effect on the energy of the state. Due to the eigenstate thermalization hypothesis, any observable will be a smooth function of the energy, and thus the small perturbation of the eigenstate produces only a small change in the entanglement entropy. In the MBL phase, since the

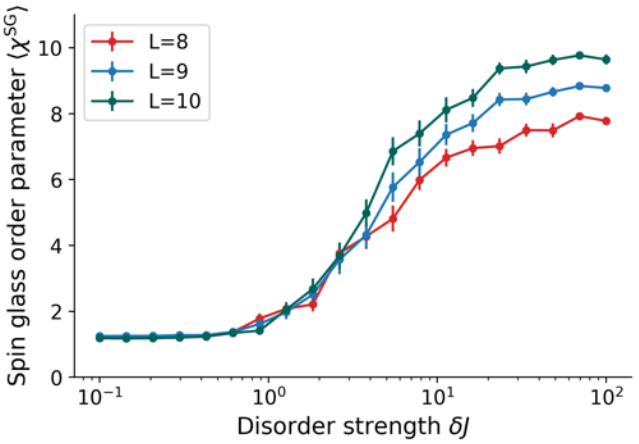

FIG. 4: The spin glass susceptibility χ_n^{SG} in the disordered transverse field Ising model as a function of disorder strength. χ_n^{SG} was computed for eigenstates near the middle of the spectrum corresponding to effectively infinite temperature, and averaged over many realizations of the quenched disorder.

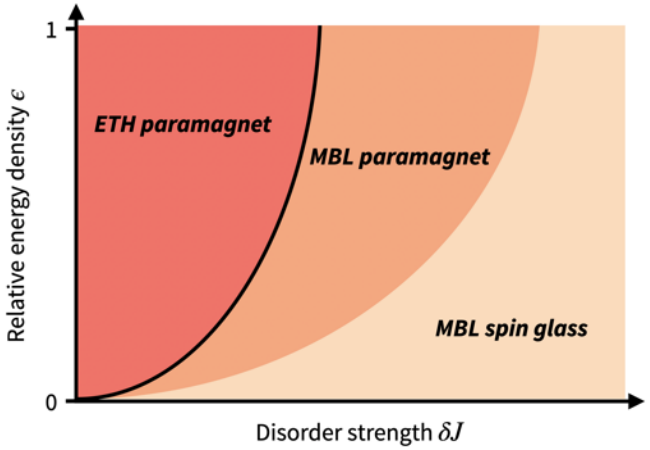

FIG. 5: A qualitative depiction of the full phase diagram[1] for the disordered transverse field Ising model. The MBL phase extends beyond the spin glass phase into the paramagnetic phase before succumbing to thermalization.

perturbation is localized and the eigenestates are also localized, the perturbation cannot propagate throughout the chain, leading to minimal generation of entanglement. On the contrary, near the MBLD transition, a small perturbation mixes thermal and localized eigenstates, with the thermal states capable of propagating the perturbation between localized states, generating substantial entanglement.

With the MBLD transition established, we now ask whether it coincides with the onset of a glassy phase. The spin glass character is probed with a generalization of the spin glass susceptibility order parameter,

$$\begin{aligned}\chi_n^{\mathrm{SG}} &= \frac{1}{L}\sum_{i,j=1}^{L} \langle n|\, \sigma_i^z \sigma_j^z\, |n\rangle^2 \\ &= 1 + \frac{1}{L}\sum_{i\neq j} \langle n|\, \sigma_i^z \sigma_j^z\, |n\rangle^2 \,, \end{aligned} \tag{17}$$

where $|n\rangle$ is an individual eigenstate of the Hamiltonian. Figure 4 demonstrates χ_n^{SG} as a function of disorder strength δJ for eigenstates near the middle of the spectrum. Indeed, we observe a clear transition from a thermal phase to a glassy phase with increasing disorder.

The full phase diagram for the model is illustrated in Fig. 5 as a function of the disorder strength δJ and energy density $\epsilon = 2(E - E_{\min})/(E_{\max} - E_{\min})$. Three distinct phases emerge,

- **ETH paramagnet**
  Labelled as simply "thermal" in the figure, in this phase the eigenstates are delocalized, the ETH is obeyed, and there is no spin glass order.

- **MBL paramagnet**
  In this phase, the disorder has become strong enough to drive the system through the MBLD transition, so that eigenstates are localized. However, the disorder is *not* sufficient to drive the spin glass transition.

- **MBL spin glass**
  For still stronger disorder, the system enters a fully disordered phase in which the eigenstates are localized and demonstrate spin glass order.

Thus, we find that the MBLD transition and spin glass transition are indeed distinct, with the MBLD transition occuring before the spin glass transition as the disorder is increased.

V. THE RANDOM ENERGY MODEL

The classical random energy model (REM) is in some sense the most disordered system that can be imagined. In words, the model consists of assigning a random energy to every configuration of the system. The energy assigned to a particular state is completely uncorrelated from the state itself and from any other energy level assigned to any other state. Due to the complete lack of correlations, the system becomes analytically simple to work with, and a direct calculation of thermodynamic quantities is very tractable. As we will derive below, the model shows a paramagnetic phase at high temperature and a "frozen" spin glass phase below a critical glass transition temperature.

The quantum random energy model (QREM) is achieved by adding a uniform transverse field the classical REM. The Hamiltonian describing the system, including the terms endowing the classical model with quantum

dynamics, is

$$H = E(\{\sigma_i^z\}) - \Gamma \sum_{i=1}^{N} \sigma_i^x. \tag{18}$$

The classical part $E(\{\sigma_i^z\})$ is a random operator of size 2^N that is diagonal in the σ^z basis. The diagonal elements are independent and identically distributed random variables with Gaussian distribution function

$$P(E) = \frac{1}{J\sqrt{\pi N}} e^{-E^2/NJ^2}, \tag{19}$$

normalized so that the energy eigenvalues of the Hamiltonian scale extensively. The transverse field $\propto \Gamma$ introduces quantum dynamics that mix classical states.

In the disordered Ising chain the spin glass character was described via an analog of the spin glass susceptibility applied to single eigenstates. This gives a detailed microscopic picture of the spin glass transition, but is not a thermodynamic quantity itself. Indeed, phases of matter need not always be defined by equilibrium thermodynamic quantities, such as the MBL phase. However, in discussing the random energy model we will move back to the familiar equilibrium setting in which phases are defined by the properties of thermodynamic *ensembles* of states rather than any individual state. In the equilibrium setting, phase transitions are marked by nonanalytic behavior of thermodynamic quantities derived from the free energy. While, in general, a direct analytical treatment of the free energy to derive the phase structure of a model can be quite difficult, it is possible for both the classical REM and QREM. We will first derive the glass transition of the classical REM, then discuss the glass transition in the QREM and find the MBLD phase transition to construct the full QREM phase diagram.

A. Classical random energy model

Here we study the thermodynamics of the classical REM, for which we set $\Gamma = 0$ in the Hamiltonian (18). To derive the free energy, we take a microcanonical route in which we consider an ensemble of states whose energy fall within a small window $E \pm \Delta E$ and denote the number of such states in this window as $n(E)$. The width of the window ΔE can be taken to be vanishingly small in the thermodynamic limit, but is required so that $n(E)$ forms a smooth function. In the thermodynamic limit, the expectation value of the number of states is simply

$$\langle n(E) \rangle_E = 2^N P(E) = \frac{\exp\left(N\left[\log(2) - (E/NJ)^2\right]\right)}{J\sqrt{\pi N}}, \tag{20}$$

where $\langle \cdot \rangle_E$ denotes an average over realizations of the random function $E(\{\sigma_i^z\})$. There are several things to notice. First, we note that fluctuations in $n(E)$ are suppressed as $1/\sqrt{N}$. This means that $n(E)$ becomes equal

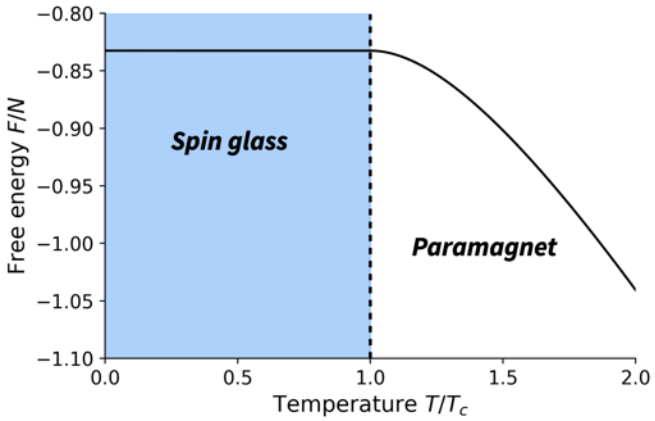

FIG. 6: The free energy of the classical REM. Below a critical temperature given in Eqn. (24), the REM freezes into a glass phase where the free energy is independent of temperature.

to its expectation value $\langle n(E) \rangle_E$ in the thermodynamic limit. Second, we see that $n(E)$ changes from exponential growth with rate $\propto N$ to exponential decay with rate $\propto N$. The crossover occurs at the critical energy

$$E_0 = NJ\sqrt{\log(2)}. \tag{21}$$

Thus, the number of states with $|E| \geq E_0$ rapidly goes to zero with increasing system size, thus we may safely restrict $n(E)$ to the interval $E \in [-E_0, E_0]$ in the thermodynamic limit. We can then use $n(E)$ to find the entropy,

$$S = k_B \log(n(E)) = N k_B \left[\log(2) - (E/NJ)^2\right]. \tag{22}$$

The entropy provides the link between the microcanonical and canonical ensembles. To find the temperature of the canonical ensemble associated with the energy E of the microcanonical ensemble, we again invoke the fundamental thermodynamic relation $1/T = dS/dE$ to find

$$T = -\frac{NJ^2}{2k_B E}, \quad (|E| < E_0). \tag{23}$$

Noting the negative sign in front, we find that only microcanonical ensembles with energy $E < 0$ correspond to physically reasonable canonical ensembles with nonnegative temperatures. Moreover, recalling that $|E|$ is bounded by E_0, only canonical ensembles down to a certain critical temperature are faithfully represented by a microcanonical ensemble. Plugging in E_0, we find the critical temperature

$$T_c = \frac{NJ^2}{2k_B E_0} = \frac{J}{2k_B\sqrt{\log 2}}. \tag{24}$$

At temperatures $T < T_c$, the energy of the associated microcanonical ensemble simply becomes railed at the lowest possible energy $-E_0$. Finally, from the definition of the free energy $F = U - TS$, where $U = 0$ above T_c

given symmetric $P(E)$, we find the free energy in terms of the temperature as,

$$F = \begin{cases} -Nk_BT\log(2) - \dfrac{NJ^2}{4k_BT} & T > T_c \\ -NJ\sqrt{\log 2} & T \leq T_c \end{cases}. \tag{25}$$

The free energy of the REM is plotted in Fig. 6, showing nonanalytic behavior at T_c, corresponding to the point in which the system freezes into a metastable state. This is precisely the spin glass phase transition. In the spin glass phase, the system exists in one of the degenerate ground states and cannot reach any of the others due to large free energy barriers. This is the breakdown of ergodicity associated with the spin glass phase transition.

B. Quantum random energy model

We now introduce quantum dynamics by setting $\Gamma > 0$. The full phase diagram for the spin glass transition was computed by Goldschmidt[8] using the replica trick. We will not derive his result here, but the phase diagram is illustrated in Fig. 7 with dashed lines corresponding to the first-order phase transitions separating the three phases, before considering where many-body localization occurs. The first two of these occur at small Γ and are the same as in the classical REM, the spin glass and classical paramagnetic phases. These are separated by the same critical temperature as in the classical REM. However, extending to larger Γ, the transverse field eventually dominates, yielding a "quantum" paramagnetic phase with ground state $|{\leftarrow}\cdots{\leftarrow}\rangle$, where $|{\leftarrow}\rangle = (|{\uparrow}\rangle + |{\downarrow}\rangle)/\sqrt{2}$.

To determine where the MBLD transition occurs, Laumann et al.[2] use spectral statistics of the Hamiltonian, in contrast to the entanglement entropy measures employed in the 1D disordered Ising chain. A reasonable argument can be given to motivate the use of spectral statistics to mark the MBL phase. In the thermal phase, the eigenstates are delocalized and the general expectation of level repulsion between energy eigenvalues for many-body interacting systems hold true. In this phase, the eigenvalues are described the Gaussian orthogonal ensemble (GOE) of random matrix theory. In typical MBL systems, the eigenstates are instead localized with exponentially small overlap. This leads to a large number of locally conserved quantities in the MBL phase that heavily constrain the dynamics. That is, with a large number of conservation laws, the Hamiltonian can be transformed into a block diagonal form via an appropriate unitary transformation, with one block for each conserved quantity. Each symmetry block only mixes states within the symmetry sector, and not between sectors. With the addition of every new symmetry sector, the complexity of the full interacting system is reduced with another sector that does not interact with the others. With enough symmetry sectors, the Hamiltonian becomes sufficiently constrained so that the remaining interactions are no longer

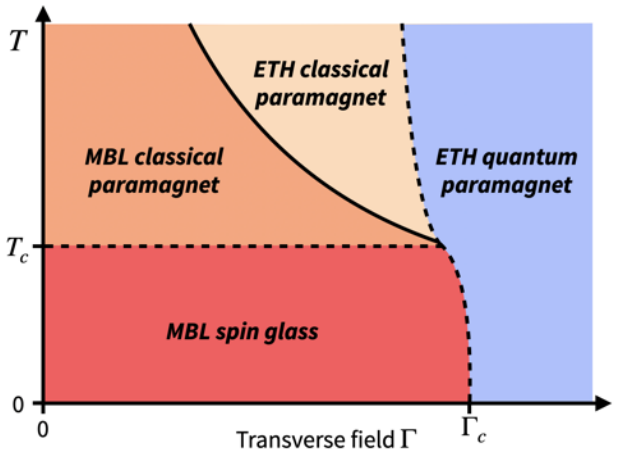

FIG. 7: The qualitative phase diagram of the QREM. Dotted lines indicate first order phase transitions computed by Goldschmidt[8], while the solid black line depicts a distinct MBLD transition found by Laumann et al.[2].

significant enough to induce level repulsion in the eigenvalues. The eigenvalues then become uncorrelated, and follow Poisson statistics.

To be more specific about spectral statistics in the MBL phase, we must discuss the nature of level spacings between energy eigenvalues for matrices described GOE random matrix theory and those with Poission eignvalue statistics. To be concrete, we consider a matrix with real eigenvalues λ_i, sorted so that $\lambda_i \geq \lambda_j$ for $i \geq j$. The level spacings between eigenvalues are then computed as $s_i = s_{i+1} - s_i \geq 0$. For GOE random matrices, the analytic form of the normalized level spacing distribution can be shown to be very close to "Wigner's surmise", given by

$$\Pr(s) = \tfrac{\pi}{2} s e^{-\pi s^2/4}. \tag{26}$$

On the other hand, if the eigenvalues are fully uncorrelated from each other then they follow Poission statistics. In this case the normalized level spacings assume a simple exponential distribution,

$$\Pr(s) = e^{-s}. \tag{27}$$

Thus, for a given Hamiltonian, the level spacing distribution provides a quantitative measure of randomness: Hamiltonians in the thermal phase follow Wigner's surmise while Hamiltonians in the MBL phase show Poisson statistics. The level spacing distribution can be further distilled into a single statistic to quantify the MBLD transition. Given the energy spacings s_i, the so-called "r statistics" (ratio) are defined as

$$r_i = \frac{\min(s_{i+1}, s_i)}{\max(s_{i+1}, s_i)}. \tag{28}$$

Both the full distribution of the r_i and their mean value $\langle r\rangle$ are useful metrics. The value for GOE random matrices is known to be close to $\langle r\rangle \approx 0.54$ and for matrices

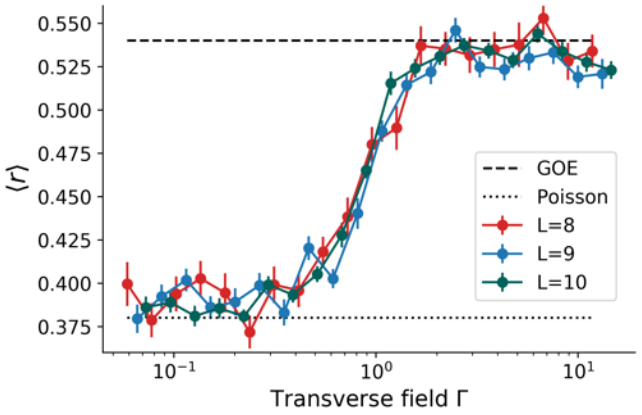

FIG. 8: The r statistic as a function of transverse field in the QREM, computed for eigenstates near the middle of the spectrum. A large number of realizations of $E\{\sigma_i^z\}$ were averaged over for each value of the transverse field. A crossover is clearly visible from Poission statistics, indicating the MBL phase, to GOE statistics, indicating the thermal phase. System sizes of 8, 9, and 10 sites were investigated.

with Poisson statistics $\langle r\rangle = 0.38$. Tunable quantum systems can exhibit a crossover between these two values going from the thermal phase to the MBL phase.

To demonstrate the MBLD transition in the QREM, we use exact diagonalization to compute the eigenvalue statistics as a function of the transverse field. The results are shown in Fig. 8, for system sizes $N = 8, 9, 10$ and for fixed $J = 1$. Eigenstates near the middle of the spectrum were used, corresponding to the high temperature limit. The r statistic indeed shows a clear transition from Poisson statistics to GOE statistics, which is presented as a marker of the MBLD transition.

Using the r statistic to locate the MBLD phase transition, Laumann et al.[2] construct the full phase diagram depicted in Fig. 7. As was seen in the 1D transverse field Ising model, a distinct MBLD transition is seen that does not coincide with the spin glass transition. The four phases are characterized as follows.

- **ETH quantum paramagnet**
  With a strong transverse field, the spins simply align with the field. The state is characterized by the ground state $|\leftarrow\cdots\leftarrow\rangle$ that dominates the free energy. Excitations above the ground state are delocalized, and the ETH is satisfied. The zero-temperature quantum phase transition to this phase occurs at a critical field strength $\Gamma_c = J\log 2$.

- **ETH classical paramagnet**
  With a weak transverse field, and at temperatures $T > T_c$, the system can enter a classical paramagnetic phase in which exponentially many states contribute to the free energy, as in a classical paramagnet. In this phase, due a combination of the transverse field mixing classical states and sufficiently high energies, the disorder is not sufficient to induce localization. That is, the eigenstates whose energies correspond to temperatures in this region obey the ETH.

- **MBL classical paramagnet**
  With a still weaker transverse field or lower temperature, the system can remain in the paramagnetic phase, but with disorder strong enough to induce localization. That is, eigenstates whose energies correspond to temperatures in this region are found to be localized.

- **MBL spin glass**
  For temperatures below the critical temperature T_c and transverse fields below the critical field Γ_c, the spin glass phase emerges. This phase is characterized by a small number of nearly degenerate ground states dominating the free energy. Low energy eigenstates falling in this region are indeed localized.

Discussion

Two models[1,2] that show both spin glass and MBL phases were reviewed. In both cases, the MBLD transition was found to be distinct from the spin glass phase transition. Thus, despite qualitative similarities, the two phases do not necessarily come hand in hand. However, a feature that was common to both models was that the spin glass phase was always accompanied by MBL, while the converse was not true. This motivates the question of whether any model of a quantum spin glass must show MBL in the glassy phase. This would be an intuitive and perhaps unsurprising result, but we leave the proof of a general statement to the interested reader.

Acknowledgments

I would like to thank Professor Vedika Khemani for her excellent lectures in many-body localization, the teaching assistants Cheryne Jonay and Jacob Marks for their hard work, and Professor Robert Laughlin for making these term papers publicly available.

[1] J. A. Kjäll, J. H. Bardarson, and F. Pollmann, Physical review letters **113**, 107204 (2014).
[2] C. R. Laumann, A. Pal, and A. Scardicchio, Physical review letters **113**, 200405 (2014).
[3] D. Sherrington and S. Kirkpatrick, Physical review letters **35**, 1792 (1975).

[4] S. F. Edwards and P. W. Anderson, Journal of Physics F: Metal Physics **5**, 965 (1975).
[5] K. Binder and A. P. Young, Reviews of Modern physics **58**, 801 (1986).
[6] P. W. Anderson, Physical review **109**, 1492 (1958).
[7] D. A. Abanin, E. Altman, I. Bloch, and M. Serbyn, Reviews of Modern Physics **91**, 021001 (2019).
[8] Y. Y. Goldschmidt, Physical Review B **41**, 4858 (1990).